Acta Cryst. (1979). A**35**, 63–72

Net Atomic Charges and Molecular Dipole Moments from Spherical-Atom X-ray Refinements, and the Relation between Atomic Charge and Shape*

By P. Coppens, T. N. Guru Row, P. Leung,
E. D. Stevens, P. J. Becker and Y. W. Yang

Department of Chemistry, State University of New York at Buffalo, Buffalo, New York 14214, *USA*

(*Received* 13 *March* 1978; *accepted* 8 *June* 1978)

Abstract

Refinement of the population and radial dependence of the spherical atomic valence shell is introduced in a general crystallographic least-squares program. The radial dependence is described by an expansion–contraction parameter κ, which, in the nine data sets tested, indicates contraction of positively and expansion of negatively charged atoms in agreement with theoretical concepts such as those incorporated in Slater's analytical rules for atomic orbitals. H atoms appear more contracted than concluded previously on the basis of a comparison of X-ray and neutron thermal parameters of sucrose. An average value of 1·40 for the radial contraction of H is used in structures for which no neutron thermal parameters are available. The resulting net charges are used to calculate X-ray molecular dipole moments whose magnitude and direction are in good agreement with theoretical and other experimental results, though some differences may be expected because of matrix effects. Net molecular charges in the one-dimensional conductor TTF–TCNQ agree with results obtained earlier by direct integration of the charge density over the molecular volume. A charge transfer from Si to V in the superconducting alloy V_3Si is also in agreement with earlier results.

Introduction

In the usual least-squares treatment of X-ray diffraction data the continuous electron density is subdivided into atomic charge densities and the basic assumptions are made that atoms are neutral and of spherical shape with a radial dependence equal to that of free atoms in the gas phase. The assumption of neutrality is, of course, at variance with a large body of theoretical and experimental work, while *X–N* and *X–X* deformation density maps attest to the asphericities of the charge distribution around bonded atoms (see, for example, Coppens, 1975*a*). Both effects may be incorporated in the X-ray scattering formalism and applications of such generalized formalisms have been described by a number of workers (Stewart, 1973; Hansen & Coppens, 1978). It is, however, possible to retain the spherical-atom approximation and allow variation of the occupancy of the valence shell (defined as the occupied canonical Hartree–Fock orbitals with the largest value of the principal quantum number), as in the *L*-shell and extended *L*-shell methods, which generally lead to atomic charges in good qualitative agreement with atomic electronegativities (Stewart, 1970; Coppens, Pautler & Griffin, 1971). But these methods have the major shortcomings that any change in the shape of the valence shell with its occupancy is not allowed for, and therefore contradict chemical theory according to which the screening of the nucleus increases with increasing electron population.

In the last four years we have applied a more flexible formalism which incorporates expansion and contraction of the atomic valence shell together with a variation of its occupancy (Griffin & Coppens, 1975; Yang, 1976; Bats & Coppens, 1977; Bats, Coppens & Koetzle, 1977; Coppens & Guru Row, 1978; Coppens, 1977). The method is less complicated than the spherical-atom multipolar expansion, yet it allows the derivation of useful information on the charge distribution and the evaluation of quantities such as molecular dipole moments. Though there are definitely minimal requirements regarding the quality of the data sets suitable for this treatment, they may be expected to be less stringent than for the aspherical-atom refinements. The 'radial' or 'monopolar' refinement therefore has potential as a routine method for the treatment of good-quality absorption-corrected data sets.

We describe here the formalism and summarize its application to a number of data sets, most of which were collected at low temperature.

Refinement with a modified spherical valence shell: the κ formalism

Expansion and contraction of the valence shell may be incorporated in the *L*-shell projection methods by the

---

* Electron Population Analysis of Accurate Diffraction Data. VII. Part VI: Hansen & Coppens (1978).

0567-7394/79/010063-10$01.00

introduction of a parameter κ which relates the perturbed valence density $\rho'_{\text{valence}}(r)$ to the free-atom ground-state density $\rho_{\text{valence}}(r)$:

$$\rho'_{\text{valence}}(r) = P_{\text{valence}}\,\kappa^3\,\rho_{\text{valence}}(\kappa r), \tag{1}$$

where P_{valence} is the valence-shell population and the factor κ^3 is required for normalization, as may be seen as follows. Since both ρ_{valence} and ρ'_{valence} are normalized to 1, we have

$$\int \rho'_{\text{valence}}(r)\,\mathrm{d}v = N\rho_{\text{valence}}(\kappa r)\,\mathrm{d}v = 1, \tag{2}$$

which gives

$$4\pi \int \rho'_{\text{valence}}(r)\,r^2\,\mathrm{d}r = 4\pi N \int \rho_{\text{valence}}(\kappa r)\,r^2\,\mathrm{d}r$$
$$= 4\pi N\,\frac{1}{\kappa^3}$$
$$\int \rho_{\text{valence}}(\kappa r)\,\kappa^2\,r^2\,\mathrm{d}\kappa r = \frac{N}{\kappa^3} = 1 \text{ or } N = \kappa^3.$$

If κ is larger than one, the valence density at r equals the free-atom valence density at a point more distant from the nucleus; thus the atom is contracted relative to the free atom and *vice versa.*

The reciprocal-space expression corresponding to (1) is:

$$F(S) = \sum_j \left[P_{j,\text{core}}\,f_{j,\text{core}}(S) + P_{j,\text{valence}}\,f'_{j,\text{valence}}(\kappa_j, S)\right]$$
$$\times \exp(2\pi i\mathbf{S}.\mathbf{r}_j)\,T_j, \tag{3}$$

where T_j is the atomic temperature factor and the P_j are the population parameters of the atom at $\mathbf{r}_j$. Note that the atomic form factors are normalized to one electron and that anomalous scattering is incorporated in the core scattering factor. The valence scattering of the perturbed atom at $S = \sin\theta/\lambda$ is given by

$$f'_{j,\text{valence}}(\kappa_j, S) = f_{j,\text{valence (free atom)}}(S/\kappa_j). \tag{4}$$

Refinement of X-ray data with κ_j and $P_{j,\text{valence}}$ as variables in addition to other structural parameters requires evaluation of derivatives such as $\partial f_{j,\text{valence}}(S, \kappa_j)/\partial \kappa_j$.

Though analytical fits to tabulated atomic form factors are available, possible inadequacies in such analytical functions may be avoided by numerical evaluation of the derivatives. This procedure is followed in a program *RADIEL*, which is a generalized version of *LINEX* 77 and allows simultaneous refinement of extinction, structural and electron density parameters.

In a further non-spherical extension we have incorporated the density formalism (1) as the leading term in a multipolar expansion of the valence density as proposed by Dawson (1967), and generalized by Stewart (1969). Though the extended formalism generally produces a better fit (with more parameters), the multipolar functions obtained in the fitting procedure are often very diffuse and have appreciable density on neighboring atoms (Coppens & Hansen, 1977; Hansen & Coppens, 1978). In this sense, they more strongly violate the requirement of locality, formulated by Kurki-Suonio (1969), which states that only electrons in the region around a nucleus should be assigned to that nucleus. The results of the extended treatment are therefore less readily analyzed in terms of charges and shapes of component atoms.

In all the refinements described here the total charge was kept constant by application of a neutrality constraint.

Table 1. *Summary of data sets*

Compound	Temperature (K)	Free-atom refinement			Radial[a] refinement			Maximum extinction factor on I	$(\sin\theta/\lambda)_{\max}$ (Å^{-1})	NO	NV[a]	Reference to data set
		$R(F)$	$R_w(F)$	S[b]	$R(F)$	$R_w(F)$	S					
Formamide (CH_3NO)	90	4·0	3·3	3·05	3·9	2·9	2·69	–	1·0	451	49	Stevens (1978)
Glycylglycine ($C_4H_8N_2O_3$)	82	4·7	3·3	2·39	4·3	2·9	2·04	0·67	1·07	2007	137	Kvick, Koetzle & Stevens (1978); Kvick, Al-Karaghouli & Koetzle (1977)
p-Nitropyridine *N*-oxide ($C_5H_4N_2O_3$)	30	3·4	3·8	1·99	3·3	3·4	1·79	0·76	1·00	1309	93	Wang, Blessing, Ross & Coppens (1976)
Ammonium thiocyanate (NH_4SCN)	81	2·0	3·3	3·30	1·7	2·6	2·60	0·86	1·00	1614	66	Bats & Coppens (1977)
TTF–TCNQ ($C_6H_4S_4.C_{12}H_4N_4$)	100	–	–	–	3·0	2·9	1·36	0·76		1006	148	Blessing & Coppens (1974)
Sulfamic acid (H_3NO_3S)	78	1·7	2·7	1·87	1·5	2·6	1·41	0·84	1·00	2181	70	Bats, Coppens & Koetzle (1977)
Sodium thiocyanate (NaSCN)	150	1·9	3·2	2·68	1·7	2·7	2·33	–	0·75	566	34	Bats & Coppens & Kvick (1977)
Potassium azide (KN_3)	300	3·0	2·0	2·90	1·8	1·3	2·07	0·75	1·25	408	17	Stevens (1977)
Vanadium silicide (V_3Si)	300	1·55	1·30	5·76	1·48	1·19	5·30	0·46	1·65	165	9	Staudenmann (1976)

(*a*) Numbers given are for treatments with isotropic H atoms and constant H κ values: see text for details.
(*b*) $R = 100[\Sigma(F_o - |F_c|)/\Sigma F_o]$; $R_w = 100\,[\Sigma\, w(F_o^2 - |F_c|^2)/\Sigma\, wF_o^2]^{1/2}$; $S = [\Sigma\, w(F_o - |F_c|)^2/(\text{NO}-\text{NV})]^{1/2}$.

Data sets

The data sets used in various parts of this analysis are summarized in Table 1. All but two of the sets were collected at liquid-nitrogen or liquid-helium temperatures (the latter in the case of *p*-nitropyridine *N*-oxide). The two exceptions are potassium azide and V_3Si, which are ionic and metallic solids respectively with small thermal-vibration amplitudes. With the exception of V_3Si (measured at the University of Geneva) all data sets were collected on the Picker automated diffractometer at the State University of New York at Buffalo. In all cases several symmetry-equivalent reflections were measured and agreement factors on F^2, calculated after correction for absorption, were typically 1–2%. Some of the data sets (especially that for V_3Si) were affected by extinction, which is incorporated in the program using the formalisms of Becker & Coppens (1975). Since both the valence charge and the κ parameter are mainly dependent on low-order reflections, extinction treatment is essential when extinction is present. Structures of some of the molecules studied and their atomic numbering are given in Fig. 1.

The treatment of H atoms. Correlation of κ and U

For the H atom which lacks the unperturbed core of the heavier atoms the radial parameter is closely correlated with the isotropic thermal-vibration parameter, the two variables being degenerate when the H density is described by a single-Gaussian distribution. In an analysis of differences between X-ray and neutron thermal parameters for sucrose, Stewart (1976) has used this single-Gaussian approximation to obtain an estimate of orbital exponents for bonded H atoms from discrepancies between X-ray and neutron vibrational parameters.

The scattering transform of a normalized single-Gaussian density function with orbital exponent $\kappa^2\alpha$ bohr^{-2} is given by

$$f = \exp\{-[2\pi^2 a_0^2/(\kappa^2\alpha)]\, S^2\}, \tag{5}$$

where $a_0 = 0{\cdot}529177$ Å bohr^{-1} and $S = \sin\theta/\lambda$.

For a thermally smeared H electron with temperature factor $B = 8\pi^2 U$ this gives

$$\langle f(1s)\rangle = \exp\{-[2\pi^2 a_0^2/(\kappa^2\alpha) + B]\, S^2\}, \tag{6a}$$

from which Stewart obtained estimates of the values of κ which would give rise to the observed discrepancies between X-ray and neutron parameters. An observed value of $\Delta B = B_{\text{X-ray}} - B_{\text{neutron}}$ of 1·7 Å^2, for example, was found to correspond to a change in κ from 1·16 to 1·23.

In our refinements we have found a change in U, corresponding to a certain error in κ, which is smaller than that calculated with expression (6*a*). This is due in part to the single-Gaussian approximation implicit in this expression. Though the atomic scattering may be approximated as a sum over several Gaussian functions an exact expression is available for the H atom:

$$\langle f(1s)\rangle = \frac{1}{[1 + (4\pi a_0 S/\kappa)^2]^2} \exp(-8\pi^2 US^2). \tag{6b}$$

As the derivative $\partial U/\partial\kappa$ which may be derived from

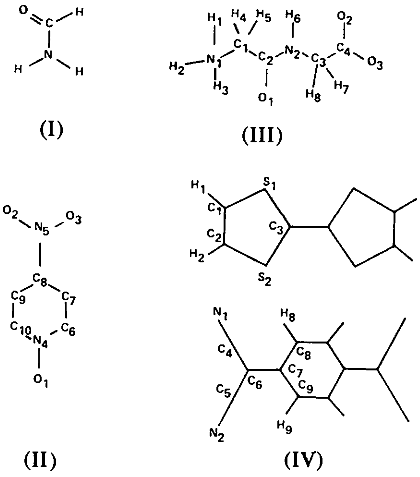

(I) (III)

(II) (IV)

Fig. 1. Diagrams and atom numbering of some of the molecules discussed in the text: (I) formamide, (II) *p*-nitropyridine *N*-oxide, (III) glycylglycine, (IV) tetrathiafulvalenium tetracyano-*p*-quinodimethanide.

Table 2. *Values of* $\partial U/\partial\kappa$ *for the* H *atom, and variation of* U_{H} *with* κ *for sulfamic acid*

(*a*) $\partial U/\partial\kappa$ for the H atom

κ	Single Gaussian $\alpha = 0{\cdot}27094809$ bohr^{-2}	Experimental H atom
1·0	0·5168	0·1399
1·1	0·3883	0·1051
1·16	0·3311	0·0896
1·2	0·2991	0·0810
1·3	0·2352	0·0637
1·4	0·1884	0·0510

(*b*) Variation of U_{H} with κ for sulfamic acid

	U (Å^2)	$\langle U\rangle$ (Å^2)	$\Delta U/\Delta\kappa$
$\kappa = 1{\cdot}35$			
H(1)	0·03505		
H(2)	0·02304	0·02938	
H(3)	0·03005		0·07
$\kappa = 1{\cdot}40$			
H(1)	0·03871		
H(2)	0·02627	0·03289	
H(3)	0·03370		

Table 3. *Net charges and κ values of glycylglycine* (82 K)

Refinements: (I) electron density and extinction parameters only;* (II) all parameters except H anisotropic thermal parameters which were kept at neutron values; (III) all parameters including H isotropic thermal parameters, $\kappa_{\rm H} = 1{\cdot}40$.

	(I)		(II)		(III)	
	q	κ	q	κ	q	κ
C(1)	−0·47 (8)	1·06 (1)	−0·42 (10)	1·02 (1)	−0·37 (10)	1·02 (1)
C(2)	0·50 (6)	1·14 (1)	0·44 (6)	1·09 (1)	0·45 (7)	1·09 (1)
C(3)	−0·37 (8)	1·08 (1)	−0·20 (9)	1·04 (1)	−0·14 (9)	1·04 (1)
C(4)	0·65 (6)	1·13 (1)	0·51 (6)	1·08 (1)	0·51 (6)	1·08 (1)
N(1)	−0·79 (7)	1·02 (1)	0·16 (11)	1·05 (1)	0·28 (11)	1·04 (1)
N(2)	−0·47 (5)	1·05 (1)	−0·41 (6)	1·01 (1)	−0·37 (6)	1·00 (1)
O(1)	−0·73 (4)	1·01 (1)	−0·54 (5)	0·99 (1)	−0·52 (5)	0·99 (1)
O(2)	−0·84 (4)	0·99 (1)	−0·61 (4)	0·99 (1)	−0·61 (4)	0·99 (1)
O(3)	−0·71 (4)	0·99 (1)	−0·68 (4)	0·97 (1)	−0·67 (4)	0·97 (1)
H(1)	0·52 (3)		0·22 (4		0·20 (4)	
H(2)	0·51 (3)	1·77 (7)	0·19 (4)	1·38 (4)	0·17 (4)	
H(3)	0·51 (3)		0·23 (4)		0·16 (4)	
H(4)	0·22 (4)		0·16 (4)		0·13 (4)	1·40
		1·50 (6)		1·36 (4)		
H(5)	0·35 (4)		0·18 (4)		0·13 (4)	
H(6)	0·39 (5)	1·51 (9)	0·31 (5)	1·43 (7)	0·17 (4)	
H(7)	0·43 (3)		0·23 (4)		0·19 (4)	
		1·56 (7)		1·41 (4)		
H(8)	0·30 (4)		0·21 (4)		0·18 (3)	
R, R_w, S	5·1, 3·8, 2·73		4·2, 2·8, 2·01		4·3, 2·9, 2·04	
NO, NV	2007, 32				2007, 141	
Dipole moments (D)	25·2 (17)		23·9 (15)		23·6 (13)	

* κ values have been constrained to be equal within each group of chemically equivalent H atoms.

(6*b*) is a function of S we have calculated the weighted average

$$\langle \partial U/\partial \kappa \rangle = \frac{\int w \partial U/\partial \kappa \, d\mathbf{S},}{\int w \, d\mathbf{S}}, \tag{7}$$

with $w = f(S)$. Results listed in Table 2(*a*) show an increased change of κ with U when an exponential rather than a Gaussian H atom is used in the calculation. We note that this implies larger values of κ for the CH H atoms in sucrose than estimated previously and this is indeed in accordance with the results described below. Temperature factors for the H atoms in sulfamic acid obtained with two different κ values show approximately the predicted dependence (Table 2*b*).

When both X-ray and neutron data are available the best κ values for the H atoms may be obtained by fixing the H thermal parameters at the neutron values. The results indicate that for both glycylglycine and sulfamic acid the H atoms are considerably contracted beyond the κ value of 1·16 quoted for the H atom in the hydrogen molecule (Stewart, Davidson & Simpson, 1965). The results for glycylglycine are especially interesting because the molecule contains both NH and CH H atoms. The κ values average about 1·40 and no clear distinction between different types of H atoms is observed (Table 3, refinement II). A similar contraction is found in sulfamic acid ($\kappa = 1{\cdot}33 \pm 3$; Table 4, refinement I). When the H positional parameters are also fixed at their neutron values the H atoms become more positive and the κ value increases even further (Table 3, refinement I). This is understandable because a hydrogen-nucleus-centered spherical-density function will be a poor representation of the H density with its centroid displaced by about 0·2 Å into the bond. To compensate for the decreased electron population on the H atoms, the N and C atoms to which the H atoms are attached become more negative, but the global charge distribution as expressed by the molecular dipole moment (Table 3) is much less affected. Nevertheless, the fit obtained in refinement (II) is much better and this latter treatment is to be preferred.

For the most common case in which no neutron data are available, the correlation between $\kappa_{\rm H}$ and $U_{\rm iso}$ prevents simultaneous refinement of these two parameters. As $\kappa_{\rm H}$ appears to be reasonably constant within its standard deviations it may be fixed at a value of 1·40 in accordance with the glycylglycine refinement results. As shown in Tables 3 and 4 this has a negligible effect on the other refinement results and gives no significant change in the overall charge distribution as expressed by the molecular dipole moment. A similar result is obtained in a sulfamic acid refinement with $\kappa_{\rm H}$ fixed at 1·35 (Table 4, refinement III).

Table 4. *Net charges and κ values of sulfamic acid*

Refinements: (I) H thermal parameters fixed at anisotropic neutron values; (II) H κ values fixed at 1·40, H thermal parameters isotropic; (III) H κ values fixed at 1·35, H thermal parameters isotropic.

	(I)		(II)		(III)	
	q	κ	q	κ	q	κ
S	0·84 (11)	1·00 (1)	0·85 (11)	1·00 (1)	0·88 (11)	1·00 (1)
O(1)	−0·43 (4)		−0·45 (4)		−0·45 (4)	
O(2)	−0·60 (4)	0·982 (2)	−0·61 (4)	0·982 (2)	−0·60 (4)	0·982 (2)
O(3)	−0·47 (4)		−0·47 (4)		−0·47 (4)	
N	0·08 (8)	1·01 (1)	0·13 (8)	1·01 (1)	0·17 (8)	1·01 (1)
H(1)	0·22 (4)		0·17 (4)		0·15 (4)	
H(2)	0·19 (4)	1·33 (3)	0·23 (4)	1·40	0·20 (4)	1·35
H(3)	0·17 (4)		0·15 (4)		0·12 (4)	
R, R_w, S	1·5, 2·6, 1·43		1·5, 2·6, 1·41		1·5, 2·6, 1·41	
NO, NV	2181, 68		2181, 70		2181, 70	
μ (D)	9·6		9·8 (6)		9·5	

Table 5. *Results for formamide*

	Experimental		Theoretical (Mulliken charge, isolated molecule)			Theoretical$^{(c)}$ (radial refinement on thermally smeared theoretical structure factors	
			(*a*)	(*b*)	(*c*)		
	q	κ	q	q	q	q	κ
O	−0·50 (4)	0·96 (1)	−0·38	−0·479	−0·602	−0·66 (3)	0·954 (3)
N	−0·71 (11)	0·97 (1)	−0·75	−0·584	−0·633	−0·76 (6)	0·971 (5)
C	0·37 (11)	1·03 (2)	0·26	0·498	0·528	0·79 (6)	1·081 (9)
H(1)	0·35 (5)		0·36	0·280	0·309	0·36 (3)	1·52 (4)
H(2)	0·37 (4)	1·40	0·37	0·300	0·327	0·37 (3)	
H(3)	0·12 (6)		0·15	−0·015	0·072	−0·10 (4)	1·34 (3)
R, R_w, S	3·9, 2·9, 2·69						
μ (D)	4·4 (0·5)		4·39	4·07	4·70	5·18	
				μ_{exp} (gas phase) = 3·71 D$^{(d)}$			

(*a*) Snyder & Basch (1972); double ζ basis set. $E = -168{\cdot}8685$ Hartree, microwave geometry.

(*b*) Christensen, Kortzeborn, Bak & Led (1970); (11,7,1/6,1) basis set contracted to (4,3,1/2,1). $E = -168{\cdot}96296$ Hartree, microwave geometry.

(*c*) Stevens, Rys & Coppens (1978); (11,5,1/6,1) basis set, contracted to (4,3,1/4,1). $E = -168{\cdot}9689$ Hartree, X-ray geometry.

(*d*) Kurland & Wilson (1957).

Accordingly the data on the other H-containing molecules were treated with κ_H fixed at 1·40. Results, listed in Tables 5–7, are generally consistent with atomic electronegativity concepts; we note, for example, that CH_2 C atoms in glycylglycine are negative while the C atoms in the carbonyl and carboxyl groups are positively charged. In comparison with the ELS-type refinement net charges are increased, which is clearly a result of the relaxation of the valence-shell shape. The relation between shape and charge and a comparison of the spherical-charge dipole moments with other values are discussed below.

Comparison of experimental results for formamide with a spherical-atom refinement of theoretical structure factors

Results for formamide are listed in Table 5 and compared with Mulliken population analyses of three theoretical calculations. The first of these is a double ζ basis set calculation by Snyder & Basch (1972) while the other two calculations are more extended and include polarization functions (Christensen, Kortzeborn, Bak & Led, 1970; Stevens, Rys & Coppens, 1978). The radial refinement agrees remarkably well with the population analyses, especially when the experimental errors and the spread among the three theoretical sets of charges are taken into account and given the differing definitions of net atomic charge. The charge density from the third theoretical calculation was used to calculate theoretical dynamic structure factors by placing the theoretical charge distribution in the experimental unit cell and applying a rigid-body thermal motion as deduced from the experimental data (Stevens, Rys & Coppens, 1977). Results of radial refinement of this data set, with thermal parameters fixed at their theoretical values, are listed in the last two columns of Table 5. Compared with the Mulliken population analysis of the same data set there is a discrepancy in the C—H group in which the H is found to be negative and the C atom is more strongly positive than indicated by the Mulliken population analysis. The κ values for C, N and O from the theoretical analysis agree well with experiment, while the average over the two types of H atoms is close to the standard value derived above from refinements using neutron diffraction information. Experimental and theoretical spherical charges agree well, except for the CH group in which the theoretical H is more negative and the C more positive than follows from experiment. Curiously the theoretical Mulliken population analysis agrees better with experiment than the theoretical spherical charges.

Comparison with direct-space integration. Results of TTF–TCNQ and V_3Si

In parallel studies (Coppens, 1975*b*; Coppens & Guru Row, 1978), we have applied a direct-space charge-integration method in which the charge in part of the crystal V is evaluated by:

$$Q = \int_{V} \rho \, \mathrm{d}t. \qquad (8)$$

When ρ is replaced by the Fourier summation over the structure factors it can be shown that expression (8) transforms into a Fourier summation in which each structure factor is multiplied by the Fourier transform of the volume of integration (Kurki-Suonio, 1971; Brown & Wilkinson, 1965, 1968; Coppens, 1977).

TTF–TCNQ

The definition of the volume of integration is least controversial when integration is to be performed over a whole molecule such as in the organic salt TTF–TCNQ, where a charge transfer of 0·47 ± 0·15 e was obtained from the data collected at 100 K.

In the κ refinement applied in the present study the molecular volume is replaced by the adjustable atomic-valence functions. Notwithstanding this difference, the κ refinement summarized in Table 7 leads to the same result as the direct-space integration. To confirm this agreement further the direct-space integration was performed over the difference density calculated *after* the κ refinement, and a residual transfer <0·01 e was found. Thus, the two very different treatments of the same data set are in excellent agreement. We conclude that the κ refinement may be used for rapid evaluation of charge transfer in multi-component molecular crystals. The comparison of the X-ray results with those from other physical measurements has been discussed elsewhere (Coppens & Guru Row, 1978).

Table 6. *Refinement of TTF–TCNQ* (100 K)

	q	κ
TTF		
C(1), C(2)	−0·03 (8)	1·08 (2)
C(3)	0·15 (9)	1·15 (3)
S(1), S(2)	−0·05 (8)	1·05 (2)
H(1), H(2)	0·12 (6)	1·25*
Sum over molecule	0·47 (15)	
TCNQ		
C(4), C(5)	0·23 (9)	1·11 (2)
C(6)	0·03 (14)	1·13 (3)
C(7)	0·04 (16)	1·11 (3)
C(8), C(9)	0·08 (9)	1·12 (2)
N(1), N(2)	−0·52 (8)	0·99 (2)
H(8), H(9)	0·05 (6)	1·25*
Sum over molecule	−0·47 (15)	

* Kept constant; this κ value is relative to the contracted H atom of Stewart, Davidson & Simpson (1965).

Table 7. *Results for p-nitropyridine N-oxide*

	q	κ
O(1)	−0·14 (6)	1·01 (1)
O(2)	−0·14 (5)	1·01 (6)
O(3)	−0·14 (5)	
N(4)	0·09 (6)	1·04 (1)
N(5)	0·42 (7)	1·06 (1)
C(6)	−0·06 (5)	1·05 (1)
C(7)	−0·16 (5)	
C(8)	−0·16 (5)	
C(9)	−0·09 (6)	
C(10)	−0·18 (5)	
H(6)	0·09 (4)	1·40
H(7)	0·16 (4)	
H(9)	0·05 (5)	
H(10)	0·25 (4)	
R, R_w, S	3·2, 3·4, 1·79	
NO, NV	1309, 93	
μ (D)	+0·4 (1·1)	

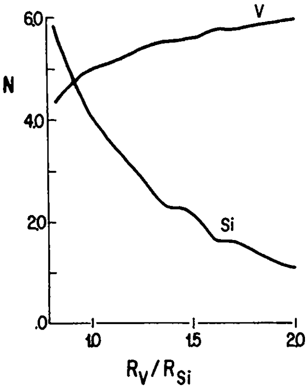

Fig. 2. Valence-electron population as a function of radius ratio defining the dimensions of the atomic polyhedra in the alloy V_3Si (from Staudenmann, Coppens & Muller, 1975).

V_3Si

In the *A*15 alloy V_3Si the direct-space integration was performed for a number of values of the radius ratio R_V/R_{Si} which determines the size of the polyhedral space-filling volumes defining each of the components. The curve of the integrated charge as a function of the radius ratio will have an approximately horizontal part when the boundary between the two volumes is in a region of low electron density and such a position may be defined as the boundary of optimum separation. The results, from Staudenmann, Coppens & Muller (1975), show the curve to be steep near atomic neutrality but much flatter in the region which corresponds to a charge transfer of 1·5–2·5 e from one Si to three V atoms (Fig. 2).

The radial parameter refinement on V_3Si is the first application to an alloy structure. Two different V core configurations were tested: the first is a 10-electron neon configuration, and the second the 18-electron Ar core; for both scattering has been tabulated (Fukamachi, 1971). The Si core was taken as the sum of the *K* and *L* shells. Results of both refinements (Table 8) indicate a transfer of 1·3 (2) e from the Si atom, in qualitative agreement with the earlier values.

Table 8. *Results for* V_3Si

A: 18-electron Ar core for V; *B*: 10-electron Ne core for V. The Si core has the 10-electron Ne configuration in both cases.

	A		*B*	
	q	κ	q	κ
V	−0·40 (8)	1·06 (3)	−0·42 (7)	1·002 (6)
Si	1·19 (24)	1·16 (7)	1·26 (22)	1·21 (8)
R, R_w, S	1·51, 1·20, 5·34		1·48, 1·19, 5·30	

Analysis of inorganic salts

A difficulty occurs in the charge-density refinement of salts of alkali halides because of the diffuseness of the valence electron of the neutral alkali metal. Its transform is therefore so compact that only a few reflections are affected by the Na valence scattering. As may be anticipated, refinement on the occupancy and κ parameters of this valence shell leads to unstable κ values with very large standard deviations. This problem does not occur for ammonium salts, and the results for NH_4SCN (Table 9) show charge transfer of almost one electron. To obtain the corresponding information for the alkali salts we have chosen the alternative and admittedly somewhat arbitrary procedure of refining on the occupancy and κ value of the next inner shell. Since the outer-shell electron scatters little it is immaterial whether or not its scattering is included in this modified valence shell. Results for KN_3 and NaSCN also listed in Table 9 suggest that the charge transfer in NaSCN is much less complete than in either NH_4SCN or KN_3. Though the results are tentative because of the valence-shell definition employed we note that a similar difference between NaSCN and NH_4SCN was found in the direct-space integration of the same data (Bats, Coppens & Kvick, 1977). Further studies are needed to clarify this point which is of importance in the understanding of ionic solids, including minerals, containing alkali halide atoms. A study combining X-ray diffraction with another technique such as X-ray photoelectron spectroscopy would be most helpful.

Calculation of 'spherical-charge' dipole moments

As the κ refinement of a molecular crystal gives a global description of the charge distribution over the molecule we may judge its success or failure by evaluating the molecular dipole moment implicit in the results. Stewart (1970) obtained a reasonable dipole moment for uracil from the results of an *L*-shell projection refinement. The possibility of deriving molecular solid-state dipole moments by such a simple technique is of further interest because differences from gas-phase values would give information on intermolecular electrostatic forces and molecular polarizabilities.

Dipole moments may also be derived from the charge distribution by numerical integration over space, or by a least-squares refinement with higher multipole density functions (Coppens & Hansen, 1977). As will

Table 9. *Net charges and* κ *values from refinements of three ionic crystals*

	NH_4SCN			NaSCN			KN_3	
	q	κ		q	κ		q	κ
S	−0·69 (6)	0·961 (7)	S	−0·39 (8)	0·92 (1)	$N_{terminal}$	−0·80 (4)	0·958 (4)
C	0·10 (6)	1·049 (7)	C	0·49 (9)	1·06 (2)	$N_{central}$	0·66 (6)	1·071 (9)
N	−0·52 (5)	0·979 (4)	N	−0·21 (7)	0·99 (1)	K	0·94 (1)	1·004 (5)
N(H)	0·92 (20)	1·08 (2)	Na	0·11 (5)	0·95 (5)			
H(1)	0·12 (5)	1·40						
H(2)	−0·05 (6)							
H(3)	0·05 (6)							
H(4)	0·08 (5)							
Ion charge (e)	1·11			0·11			0·94	

Table 10. *Comparison of magnitudes of experimental and theoretical dipole moments* (D)

	X-ray data (κ refinement)	Theoretical	Other experimental values
Sulfamic acid (78 K)	9·6 (6)	9·33(a)	10·2(b)(i) 12·2(b)(ii) 13·3(b)(iii)
Formamide (90 K)	4·4 (5)	4·3(c) 4·07(d)	3·9(e)(iv)
Glycylglycine (82 K)	23·6 (1·3)		27·8(f)(v)
p-Nitropyridine *N*-oxide	0·4 (1·0)		0·69(g)(vi)
SCN^- in NH_4SCN	0·8 (4)		
SCN^- in NaSCN	1·3 (6)		

(*a*) J. Rys, 4-31G, unpublished results; (*b*) Sears, Fortune & Blumenshine (1966), (*c*) Snyder & Basch (1972), double ζ; (*d*) Christensen, Kortzeborn, Bak & Led (1970); (*e*) Kurland & Wilson (1957); (*f*) Aaron & Grant (1967), Aaron, Grant & Young (1966); (*g*) Katritzky, Randall & Sutton (1957).
(i) In dimethyl sulfoxide; (ii) in *N*-methylpyrrolidine; (iii) in *N*,*N*-dimethylacetamide; (iv) gas phase; (v) in H_2O; (vi) in benzene.

be discussed in detail elsewhere, general agreement is obtained between the κ refinement dipole moments and those from the alternative and more sophisticated methods.

Spherical-charge dipole moments for a number of molecules and ions are listed in Table 10. Those for the SCN^- ion are with respect to an origin at the ionic center of mass, while the dipole moments for the neutral molecules are origin independent. In the case of H atoms the positive charge of the proton was located at the neutron diffraction position or, lacking this information, at the H positions determined in a high-order refinement, while negative charge was centered at the locations from the X-ray κ refinement. Thus the expression used is

$$\mathbf{u} = \sum_i q_i \mathbf{r}_i + \sum_{\text{H atoms}} (P_i \mathbf{r}_i - \mathbf{R}_i), \qquad (9)$$

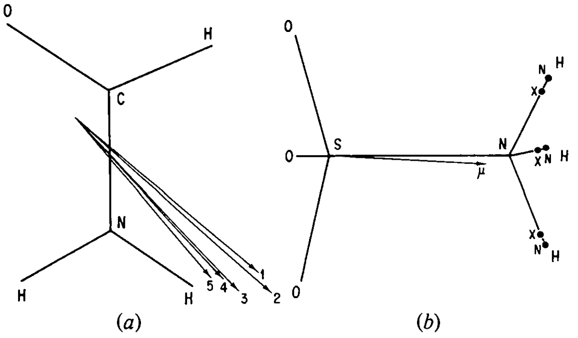

Fig. 3. (*a*) Direction and magnitude of the dipole moment of formamide from various sources (for numerical information see Table 5). [(1) X-ray spherical atom. (2) X-ray aspherical atom. (3) Theory, double ζ. (4) Theory, extended basis. (5) Microwave.] (*b*) Direction and magnitude of the spherical-charge dipole moment in sulfamic acid. The H X-ray and neutron positions are marked by *X* and *N* respectively.

where the first sum is over the non-hydrogen atoms, q_i is the net charge on atom *i*, and P_i is the electron population on the *i*th H atom. The X-ray atomic and H nuclear positions are defined by the vectors $\mathbf{r}_i$ and $\mathbf{R}_i$ respectively.

The experimental values for sulfamic acid and formamide are close to theoretical results for the isolated molecule, especially when standard deviations estimated (as described below) at 0·5–0·6 D are taken into account. For both sulfamic acid and glycylglycine solid-state values are appreciably lower than dipole moments measured in solution. Since the theoretical value for sulfamic acid agrees with the X-ray result, this may represent a real difference between the different phases. For formamide the X-ray value (and the theoretical values) are larger than the gas-phase microwave measurement, but the discrepancy is smaller and perhaps not significant. The same is true for *p*-nitropyridine *N*-oxide.

In addition to the magnitude we may compare the calculated and measured directions of the dipole moments. Formamide is an especially interesting case because the direction of the dipole moment in the isolated molecule has also been measured in the microwave experiment. Results are shown in Fig. 3(*a*) and Table 11, which also include the X-ray dipole moment from the aspherical-atom least-squares refinement. The directions and magnitudes of the two X-ray moments are in good agreement indicating the adequacy of the spherical κ approximation as a means of deriving semi-quantitative dipole moments.

Relative to the two theoretical vectors, which are practically parallel, the X-ray moments make a larger angle with the CN bond direction. The angle with the microwave dipole moment is even larger, though the total spread is less than 10°, certainly an indication that dipole moments and their directions may be derived from X-ray diffraction measurements.

One may attempt to assign the difference in direction

Table 11. *Comparison of formamide dipole moments* (μ) *and angles with the* C—N *axis* (α)

	μ (D)	α (°)	Reference
Theoretical			
Double ζ	4·39	42·6	Snyder & Basch (1972)
Extended basis (I)	4·07	41·9	Christensen, Kortzeborn, Bak & Led (1970)
Extended basis (II)	4·70	40·4	Stevens, Rye & Coppens (1978)
Experimental			
X-ray:			
spherical atom	4·4 (5)	49·0 (1·3)	This work
aspherical atom	4·8 (5)	47·6 (1·3)	To be published
Microwave	3·71	39·6	Kurland & Wilson (1957)

to the effect of neighboring molecules on the molecular charge distribution, but such an assignment must await the accumulation of further experimental evidence. Of the other molecules listed in Table 10, the dipole is closely directed along SN in sulfamic acid (Fig. 3*b*) and from the carboxyl to the ammonio group in glycylglycine. In *p*-nitropyridine *N*-oxide the X-ray dipole moment is small and its direction therefore poorly determined, even though the result listed in Table 10 is closely aligned with the molecular axis.

Estimate of errors in the experimental dipole moment

The accuracy of the X-ray dipole moments is affected by errors in the net charges q_i and P_i and the atomic positions $\mathbf{r}_i$ and $\mathbf{R}_i$ as defined in expression (9). If $\mathbf{M}$ represents the $m \times m$ variance–covariance matrix for these parameters and $\mathbf{T}$ is a $3 \times m$ matrix defined by $T_{ij} = \partial\mu_i^C/\partial p_j$, where μ_i^C are the components of $\boldsymbol{\mu}$ along the crystal axes and p_j the parameters described above, the variances and covariances of the components of $\boldsymbol{\mu}$ are obtained from

$$\mathbf{M}_\mu^C = \mathbf{TMT}^T. \qquad (11)$$

It is often of interest to transform $\mathbf{M}_\mu^C$ to a molecular coordinate system so that errors in angles with the molecular axes may be evaluated. This can be accomplished by replacing $T_{ij} = \partial\mu_i^C/\partial p_j$ in expression (11) with the corresponding derivatives of the components of $\boldsymbol{\mu}$ in the molecular coordinate system. If the transformation of coordinates from the crystal to the molecular coordinate system is described by

$$\mathbf{x}^M = \mathbf{A}(\mathbf{x}^C - \mathbf{B}),$$

where the vector $\mathbf{B}$ represents a shift in origin between the two coordinate systems, then

$$\boldsymbol{\mu}^M = \mathbf{A}\boldsymbol{\mu}^C - \mathbf{AB}\sum_i q_i. \qquad (12)$$

For a neutral molecule $\sum_i q_i$ equals zero and

$$\frac{\partial\boldsymbol{\mu}^M}{\partial p_i} = \mathbf{A}\,\frac{\partial\boldsymbol{\mu}^C}{\partial p_i}. \qquad (13)$$

Error estimates given in Tables 10 and 11 are evaluated in this way. The most important contributions are from the uncertainties in the net charges and the X-ray H positions.

The relation between atomic charge and shape

Because of electron–electron repulsions the radial dependence of the atomic valence density is expected to be a function of the electron population of the atom. This dependence is implicit in Slater's rules for analytical atomic orbitals, the radial part of which is described by $\Phi = N\exp[-(Z - S)r/c]$, where N is a normalization factor, $c = 2$ for first-row atoms, Z is the nuclear charge and S is a screening factor which increases with increasing number of electrons (see, for example, Coulson, 1961). An additional electron in the L shell of a C or N atom, for example, increases S by 0·35 and, therefore, decreases the exponent $(Z - S)/2$ by 0·175 (a.u.)$^{-1}$, or, in the terminology of the present study, decreases κ by a fraction $0{\cdot}175/(Z - S)$.

The relation between κ and q is best studied for the N atom, which in the molecules analyzed here displays a wide range of net charges (Fig. 4). Extremes are found in the azide ion in which the terminal atoms bear a net negative charge of −0·80 (4) e, while the central atom is positive by 0·66 (6) charge units. The N atom in the ammonium group appears to be even more positive, but its charge is unusually strongly correlated with those of the surrounding four H atoms which act as a pseudo-spherical density function. The error in the N charge (point *h* in Fig. 4) is therefore large, even though the

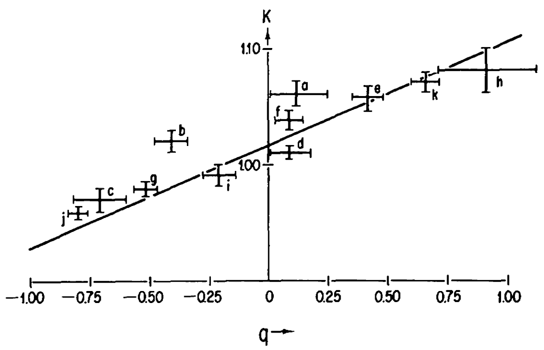

Fig. 4. Relation between κ and q (net charge) for N atoms in a number of structures: (*a*), (*b*) glycylglycine, (*c*) formamide, (*d*), (*e*) *p*-nitropyridine *N*-oxide, (*f*) sulfamic acid, (*g*), (*h*) NH_4SCN, (*i*) NaSCN, (*j*), (*k*) KN_3. Bars indicate estimated standard deviations.

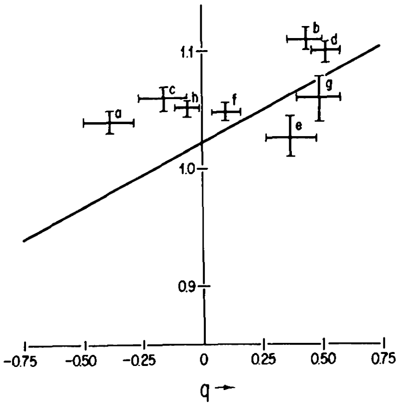

Fig. 5. As Fig. 4 for C atoms: (*a*), (*b*), (*c*), (*d*) glycylglycine, (*e*) formamide, (*f*) NH_4SCN, (*g*) NaSCN, (*h*) *p*-nitropyridine *N*-oxide.

total net charge on the ammonium group is much better determined.

The full line in Fig. 4 has the slope predicted by Slater's rules and a κ value at zero net charge which is the ratio of the exponent as given by these rules and the best 'single ζ' values for atomic orbitals given by Clementi & Raimondi (1963) (a weighted average over the $2s$ and $2p$ values was taken in the latter case). Thus, Slater's rules predict the neutral bonded atom to be slightly contracted, a prediction which is in good agreement with the X-ray evidence presented here. We note that such a contraction is commonly incorporated in the X-ray scattering formalism for H when the scattering factor of Stewart, Davidson & Simpson (1965) is used. The data reported here show that both expansion and contraction of the first-row-atom valence shell should be allowed for in the X-ray scattering formalism. The amount of contraction per unit change in net charge for N is in remarkable agreement with Slater's prediction.

A similar curve for C is given in Fig. 5. The number of points and the range of net charges are smaller than for N and the results are much less conclusive than for N. In particular, the point for formamide appears to be low. The scatter of the points may well be related to the uniform assignment of a κ value of 1·4 to the radial parameter of H, which may bias the parameters of the adjacent C atom. If the points for glycylglycine only are considered (a, b, c and d), which are from the refinement with neutron thermal parameters for the H atoms (column II, Table 3), a much clearer correlation is observed, with a slope slightly less than that given by the Slater curve. Further discussion of the C atom κ/q curve must be delayed until more points become available.

The authors would like to thank Dr R. F. Stewart for helpful comments. Support of this work by the National Science Foundation (CHE 7613342A01) is gratefully acknowledged.

References

AARON, M. W. & GRANT, E. H. (1967). *Trans. Faraday Soc.* **63**, 277–280.

AARON, M. W., GRANT, E. H. & YOUNG, S. E. (1966). *Chem. Soc. Spec. Publ.* **20**, 77–82.

BATS, J. W. & COPPENS, P. (1977). *Acta Cryst.* B**33**, 1542–1548.

BATS, J. W., COPPENS, P. & KOETZLE, T. F. (1977). *Acta Cryst.* B**33**, 37–45.

BATS, J. W., COPPENS, P. & KVICK, A. (1977). *Acta Cryst.* B**33**, 1534–1542.

BECKER, P. J. & COPPENS, P. (1975). *Acta Cryst.* A**31**, 417–425.

BLESSING, R. H. & COPPENS, P. (1974). *Solid State Commun.* **15**, 215–221.

BROWN, P. J. & WILKINSON, C. (1965). *Acta Cryst.* **18**, 398–400.

BROWN, P. J. & WILKINSON, C. (1968). *Acta Cryst.* A**24**, 347–348.

CHRISTENSEN, D. H., KORTZEBORN, R. N., BAK, B. & LED, J. J. (1970). *J. Chem. Phys.* **53**, 3912–3922.

CLEMENTI, E. & RAIMONDI, D. L. (1963). *J. Chem. Phys.* **38**, 2686–2689.

COPPENS, P. (1975*a*). *MTP International Review of Science. Physical Chemistry, Series* 2. Vol. 11, edited by J. M. ROBERTSON, pp. 21–54. London: Butterworths.

COPPENS, P. (1975*b*). *Phys. Rev. Lett.* **34**, 98–100.

COPPENS, P. (1977). *Isr. J. Chem.* **16**, 159–162.

COPPENS, P. & GURU ROW, T. N. (1978). *Proc. NY Acad. Sci.* In the press.

COPPENS, P. & HANSEN, N. K. (1977). *Isr. J. Chem.* **16**, 163–165.

COPPENS, P., PAUTLER, D. & GRIFFIN, J. F. (1971). *J. Am. Chem. Soc.* **93**, 1051–1058.

COULSON, C. A. (1961). *Valence*, 2nd edition. Oxford Univ. Press.

DAWSON, B. (1967). *Proc. R. Soc. London Ser. A*, **298**, 255–263.

FUKAMACHI, T. (1971). *Mean X-ray Scattering Factors Calculated from Analytical Roothaan–Hartree–Fock Wave Functions by Clementi.* Tech. Rep. Ser. *B*, No. 12, Institute for Solid State Physics, Univ. of Tokyo.

GRIFFIN, J. F. & COPPENS, P. (1975). *J. Am. Chem. Soc.* **97**, 3496–3505.

HANSEN, N. K. & COPPENS, P. (1978). *Acta Cryst.* A**34**, 909–921.

KATRITZKY, A. R., RANDALL, E. W. & SUTTON, L. E. (1957). *J. Chem. Soc.* pp. 1769–1775.

KURKI-SUONIO, K. (1969). *Acta Cryst.* A**25**, S85.

KURKI-SUONIO, K. (1971). *Analysis of Crystal Atoms on the Basis of X-ray Diffraction.* Ital. Crystallogr. Assoc. Meet., Bari, Italy.

KURLAND, R. J. & WILSON, E. B. JR (1957). *J. Chem. Phys.* **27**, 585–590.

KVICK, A., AL-KARAGHOULI, A. R. & KOETZLE, T. F. (1977). *Acta Cryst.* B**33**, 3796–3801.

KVICK, A., KOETZLE, T. F. & STEVENS, E. D. (1978). To be published.

SEARS, P. G., FORTUNE, W. H. & BLUMENSHINE, R. L. (1966). *J. Chem. Eng. Data*, **11**, 406–409.

SNYDER, L. C. & BASCH, H. (1972). *Molecular Wave Functions and Properties.* New York: John Wiley.

STAUDENMANN, J. L. (1976). Thesis, Univ. of Geneva.

STAUDENMANN, J. L., COPPENS, P. & MULLER, J. (1975). *Solid State Commun.* **19**, 29–33.

STEVENS, E. D. (1977). *Acta Cryst.* A**33**, 580–584.

STEVENS, E. D. (1978). *Acta Cryst.* B**34**, 544–551.

STEVENS, E. D., RYS, J. & COPPENS, P. (1977). *Acta Cryst.* A**33**, 333–338.

STEVENS, E. D., RYS, J. & COPPENS, P. (1978). *J. Am. Chem. Soc.* **100**, 2324–2329.

STEWART, R. F. (1969). *J. Chem. Phys.* **51**, 4569.

STEWART, R. F. (1970). *J. Chem. Phys.* **53**, 205–213.

STEWART, R. F. (1973). *J. Chem. Phys.* **58**, 4430–4438.

STEWART, R. F. (1976). *Acta Cryst.* A**32**, 182–185.

STEWART, R. F., DAVIDSON, E. R. & SIMPSON, W. T. (1965). *J. Chem. Phys.* **42**, 3175–3187.

WANG, Y., BLESSING, R. H., ROSS, F. K. & COPPENS, P. (1976). *Acta Cryst.* B**32**, 572–578.

YANG, W. Y. (1976). Thesis, State Univ. of New York at Buffalo.